

1982

Direct Monte Carlo Simulation of kV Electron Scattering Processes-N(E) Spectra for Aluminum

Ryuichi Shimizu
Osaka University Suita-shi

Shingo Ichimura
Osaka University Suita-shi

Follow this and additional works at: <https://digitalcommons.usu.edu/electron>

 Part of the [Biology Commons](#)

Recommended Citation

Shimizu, Ryuichi and Ichimura, Shingo (1982) "Direct Monte Carlo Simulation of kV Electron Scattering Processes-N(E) Spectra for Aluminum," *Scanning Electron Microscopy*: Vol. 1982 : No. 1 , Article 14.
Available at: <https://digitalcommons.usu.edu/electron/vol1982/iss1/14>

This Article is brought to you for free and open access by the Western Dairy Center at DigitalCommons@USU. It has been accepted for inclusion in Scanning Electron Microscopy by an authorized administrator of DigitalCommons@USU. For more information, please contact digitalcommons@usu.edu.



DIRECT MONTE CARLO SIMULATION OF kV ELECTRON SCATTERING PROCESSES – N(E) SPECTRA FOR ALUMINUM

Ryuichi Shimizu and Shingo Ichimura

Department of Applied Physics, Osaka University
Suita-shi, Yamadaoka 2-1, Osaka, Japan 565
Phone: 06-877-5111, ext. 46558

ABSTRACT

A Monte Carlo simulation of the scattering processes of kV electrons penetrating into aluminum was performed. The simulation is based on the use of different types of differential cross-sections for individual elastic and inelastic scattering: (i) the differential cross-sections derived by the partial wave expansion method for elastic scattering, (ii) Gryzinski's excitation function for inner-shell electron excitation, (iii) Streitwolf's excitation function for conduction electron excitation, (iv) Quinn's mean free path for plasmon excitation.

The main purpose of this work is to see how accurately the present direct Monte Carlo simulation describes the backscattered electrons from Al, which is the most important factor for making quantitative Auger electron spectroscopy more reliable.

The calculations were done for incident electron energies of 1.5 and 3 keV at angles of incidence 0° (normal) and 45° , respectively. Experiments were also performed using two Auger Scanning Electron Microscopes (SEM) JAMP-10 (for normal incidence) and JAMP-3 (for 45° incidence) to verify the theoretical calculations with comparison of N(E)-spectra.

The results show satisfactory agreement between theory and experiment. This suggests that the present direct Monte Carlo simulation describes the scattering processes of kV electrons in aluminum and the background intensity in Auger electron spectroscopy with considerable accuracy.

Keywords: Monte Carlo simulation, N(E)-spectra, Inelastic Scattering, Backscattered electrons, Auger electron spectroscopy, conduction-electron excitation, inner-shell-electron excitation, plasmon excitation.

INTRODUCTION

A Monte Carlo approach to the direct simulation of the scattering of electrons in aluminum was proposed by Shimizu et al. (1976) several years ago. In this approach the scattering processes consist of elastic and inelastic scattering; furthermore, inelastic scattering is separated into three elementary excitation processes (conduction-electron, plasmon and L-shell electron excitations).

The theoretical stopping powers for those processes were used instead of Bethe's stopping power equation to describe the inelastic scattering processes and the electron penetration. Simulations based on this approach satisfactorily describe the energy as well as the angular distribution of the transmitted electrons penetrating through thin aluminum films.

Thus, this direct Monte Carlo simulation approach has been confirmed to be useful for the theoretical description of electron penetration of kV electrons at rather high energies (beyond 10 keV). The extension of this approach to lower energy regions, particularly to backscattered electrons, however, was not done because the screened Rutherford scattering formula, used to describe elastic scattering, is no longer valid for the lower energy region below several kilovolts even for aluminum.

With the recent rapid increase in applications of Auger electron spectroscopy (AES), a precise knowledge of the scattering processes of penetrating electrons with kinetic energies below few keV is now required. Particularly, an understanding of both the contribution to Auger electron generation and background formation in AES by backscattered electrons is very important for performing quantitative Auger analysis.

Recently a computer program for numerical calculation of precise differential cross-sections for elastic scattering by the partial wave expansion method, written by Yamazaki (1977), now allows us to use this elastic scattering cross-section instead of the screened Rutherford scattering formula in the direct Monte Carlo simulation.

The present study aims at verifying the direct Monte Carlo simulation approach based on uses of (i) elastic scattering cross-sections derived by partial wave expansion method and (ii) three different theoretical expressions for inelastic scattering; Streitwolf's (1959) excitation function for conduction electron-excitation, Quinn's (1962) expression for plasmon-excitation, and Gryzinski's (1965) excitation function for L-shell electron excitation.

This approach was applied to electron backscattering phenomena, particularly the $N(E)$ -spectra in AES for comparison with experiment. The results show very good agreement, suggesting that the present direct Monte Carlo approach is useful for a theoretical description of electron scattering, leading to a sounder basis for quantitative Auger analysis.

BASIC MODEL FOR ELECTRON SCATTERING

The present Monte Carlo simulation is, in principle, the same as that proposed by Shimizu et al. (1976) except for the use of a differential cross-section for elastic scattering derived from the partial wave expansion method instead of the Rutherford formula. Only an outline of the treatment of scattering processes in this approach is, therefore, described below.

Elastic scattering

In the present simulation we used the differential cross-sections for elastic scattering, which were obtained from numerical calculations by the partial wave expansion method (PWEM). Details of those calculations have been described elsewhere (Ichimura and Shimizu, 1981). The differential cross-section, $d\sigma^{el}(\theta)/d\theta$, for elastic scattering is given by the following equation:

$$\frac{d\sigma^{el}(\theta)}{d\theta} = |f(\theta)|^2 + |g(\theta)|^2 \quad (1)$$

Here, θ denotes the scattering angle, and the scattering amplitudes $f(\theta)$ and $g(\theta)$ are obtained by the partial wave expansion method (PWEM).

The calculations $d\sigma^{el}(\theta)/d\theta$ were done at 100 eV intervals from 100 eV to the primary energy for 1.5 kV; and at 100 eV, 200 eV and 400 eV intervals from 400 eV to the primary energy of 3.0 keV. The values between them were interpolated.

Inelastic scattering

The theoretical expressions of the stopping powers for the elementary excitation processes, the summation of which gives a stopping power equivalent to Bethe's equation, were proposed by Ritchie et al. (1969) for aluminum. They have shown that the Bethe's stopping power is obtained by the summation of the theoretical stopping powers for: (i) conduction electrons, derived from the electron gas model, (ii) plasmons, derived from dielectric theory, and (iii) L-shell electrons given by Gryzinski's theory. Shimizu et al. (1976) used the theoretical stopping power for (i) conduction electrons given by Streitwolf, (ii) plasmons from Quinn's equation, and (iii) L-shell electrons from Gryzinski's equation. Recently Ashley et al. (1979) proposed other theoretical stopping powers derived from the electron gas dielectric function for free electron and Manson's atomic generalized oscillator strengths for inner-shell ionization. Those stopping powers are plotted in Fig. 1 for comparison. Although it seems that a fairly large discrepancy exists between the theoretical stopping powers for free electrons, there are no substantial differences between those theoretical stopping powers for both the free electron and inner-shell electron ex-

LIST OF SYMBOLS

E_p	= Primary energy of an incident electron.
E_j	= Binding energy of j-shell electrons.
E_F	= Fermi's energy.
ΔE	= Energy transferred to a conduction electron or core electron through simple electron excitation process. (In the figures ΔE denotes energy window of an energy analyzer.)
P	= Momentum
ϵ	= Electric charge
m	= Electronic mass
a_0	= Bohr radius
n	= Free electron density
n_j	= Number of j-shell electrons
ω_p	= Plasma frequency
λ_p	= Mean free path for plasmon excitation.
$\frac{d\sigma_c(\Delta E)}{d(\Delta E)}$	= Excitation function for core-electron.
$\frac{d\sigma^{el}(\theta)}{d\theta}$	= Differential cross-section for elastic scattering.
$f(\theta), g(\theta)$	= Scattering amplitudes derived by partial wave expansion method.
$N(E)$	= Energy distribution of backscattered electrons.
η	= Backscattering factor.

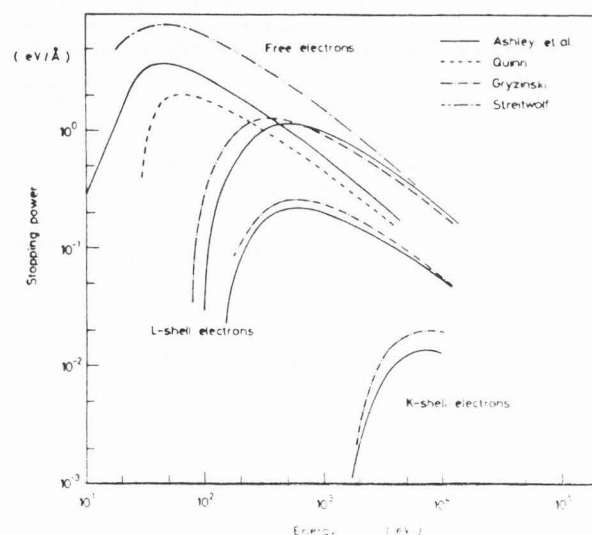


Fig. 1. Theoretical stopping powers for elementary excitations in aluminum.

citations. In this simulation therefore, we used the Streitwolf's excitation function for conduction electrons, Quinn's mean free path for plasmons, and Gryzinski's excitation function for L-shell electrons. A significant advantage of the use of these excitation functions is their capability to describe the secondary electrons generated by the single electron excitation. Those secondary electrons of high energy are a significant source of Auger electrons. The form of the equations used is as follows:

Theoretical N(E) Spectra for Aluminum

(i) Excitation function for conduction-electron (Streitwolf, 1959)

$$\frac{d\sigma_c(\Delta E)}{d(\Delta E)} = \frac{\epsilon^4 k_F^3}{3\pi E_p (\Delta E - E_F)^2}$$

for $\Delta E > E_F$ (2)

$$\text{and } \frac{d\sigma_c(E_r)}{d(\Delta E)} = \frac{0.34 \epsilon^4 k_F^3}{3\pi E_p E_F^2}$$

for $\Delta E \leq E_F$

(ii) Excitation functions for inner-shell electrons (Gryzinski, 1966)

$$\frac{d\sigma_j(\Delta E)}{d(\Delta E)} = \frac{\pi \epsilon^4 n_j}{(\Delta E)^2} \frac{1}{\Delta E} \left(\frac{E_p}{E_p + E_j} \right)^{3/2} \cdot \frac{E_j}{E_p} \cdot \left(1 - \frac{\Delta E}{E_p} \right)^{E_j/(E_j + \Delta E)} \cdot \left\{ \frac{\Delta E}{E_j} \left(1 - \frac{E_j}{E_p} \right) + \frac{4}{3} [\ln 2.7 + \left(\frac{E - \Delta E}{E_j} \right)^{1/2}] \right\}$$

(3)

The angular deflection of a primary electron after the above single electron excitation is given from the classical binary encounter model as

$$\sin^2 \theta = \Delta E / E$$

(4)

(iii) Mean free path for plasmon excitation (Quinn)

$$\lambda_p = \frac{2 a_0}{\omega_p} E \ln \left[\frac{(P^2 + 2m\omega_p)^{1/2} - P_F}{P - (P^2 - 2m\omega_p)^{1/2}} \right]$$

(5)

$$P = (2mE)^{1/2} \quad P_F = (2mE_F)^{1/2}$$

(6)

The angular differential cross-section is given as

$$\frac{d}{d\theta} \sigma_p(\theta) = \frac{1}{2\pi n a_0} \frac{\theta_E}{\theta^2 + \theta_E^2}, \quad \theta_E = \frac{\hbar \omega_p}{2E}$$

(7)

The calculation procedures using uniform random numbers were described in detail by Shimizu et al., 1976.

RESULTS

Calculations were performed for 1.5 and 3.0 kV electrons incident on aluminum at angles of incidence 0° (normal in-

cidence) and 45°, respectively. All the Monte Carlo results were obtained from 200,000 electron trajectories. Energy distributions of backscattered electrons from an aluminum target are shown in Figure 2(a) and (b), for angles of incidence 0° and 45°. Histograms shows $d\eta/dE$ or the N(E)-spectrum with an energy interval of 2.5 eV for $E_p = 1.5$ keV and 5.0 eV for $E_p = 3.0$ keV. In the figures one can clearly see up to six plasma loss peaks above the background.

In practice, energy spectra were measured by an analyzer with an energy window ΔE , which determines the energy resolution of the measured N(E)-spectrum. The calculated spectrum may be matched to the experimental spectrum simply by convoluting the calculated spectrum (Fig. 2) with a Gaussian distribution function to represent the instrumental resolution function.

This convolution was made for different values of energy window, ΔE , and the results are shown in Fig. 3 and 4. Those figures visualize how the energy resolution in energy loss spectroscopy deteriorates as the energy window becomes broader, i.e., for larger ΔE .

For an incident beam energy of 1.5 keV the plasmon peaks are still resolved even for the energy window, $\Delta E/E = 0.6\%$, but these peaks are no longer visible even for an energy window of 0.4% at 3 keV incident beam energy.

COMPARISON WITH EXPERIMENT

The energy spectrum of the backscattered electrons measured with an energy analyzer, i.e., cylindrical mirror analyzer (CMA), is not the N(E)-spectrum as shown in Fig. 2, but the E N(E)-spectrum owing to proportionality of the energy window of the analyzer to the kinetic energy of electrons. Hence the N(E)-spectrum shown in Fig. 2 can not be directly compared with the experimental results obtained by AES with CMA.

We have therefore multiplied the N(E)-spectrum of Fig. 2 by E to get the E N(E)-spectrum for comparison with experiment. In Figures 5-8, we compare the theoretical E N(E)-spectra with the corresponding experimental results obtained from JEOL commercial Auger-SEM's, a JAMP-10 (for normal incidence) and a JAMP-3 for angle of incidence of 45°.

The theoretical E N(E)-spectra were plotted by choosing an appropriate vertical scale in the ordinate so that the intensities of the E N(E)-spectra match the experimental ones. The loss spectrum in high energy region is also shown for $E_p = 1.5$ keV on an enlarged scale in each spectrum for a more detailed examination of agreement between theory and experiment. Those theoretical energy loss spectra were obtained for an energy window, $\Delta E/E = 0.5\%$, used in all the experimental measurements. The results clearly indicate that the present direct Monte Carlo simulation describes the experiment with considerable accuracy. We may therefore conclude, from those comparisons, that direct Monte Carlo simulation is a useful technique for understanding electron-penetration and backscattering phenomena, and should enable quantitative AES to be improved. More basic theoretical data on the elementary excitation in other materials is required before the direct Monte Carlo simulation approach can be extended to a wider range of materials to give a more comprehensive understanding of the complicated scattering processes of kV electrons in solids.

N(E) Spectra for Al

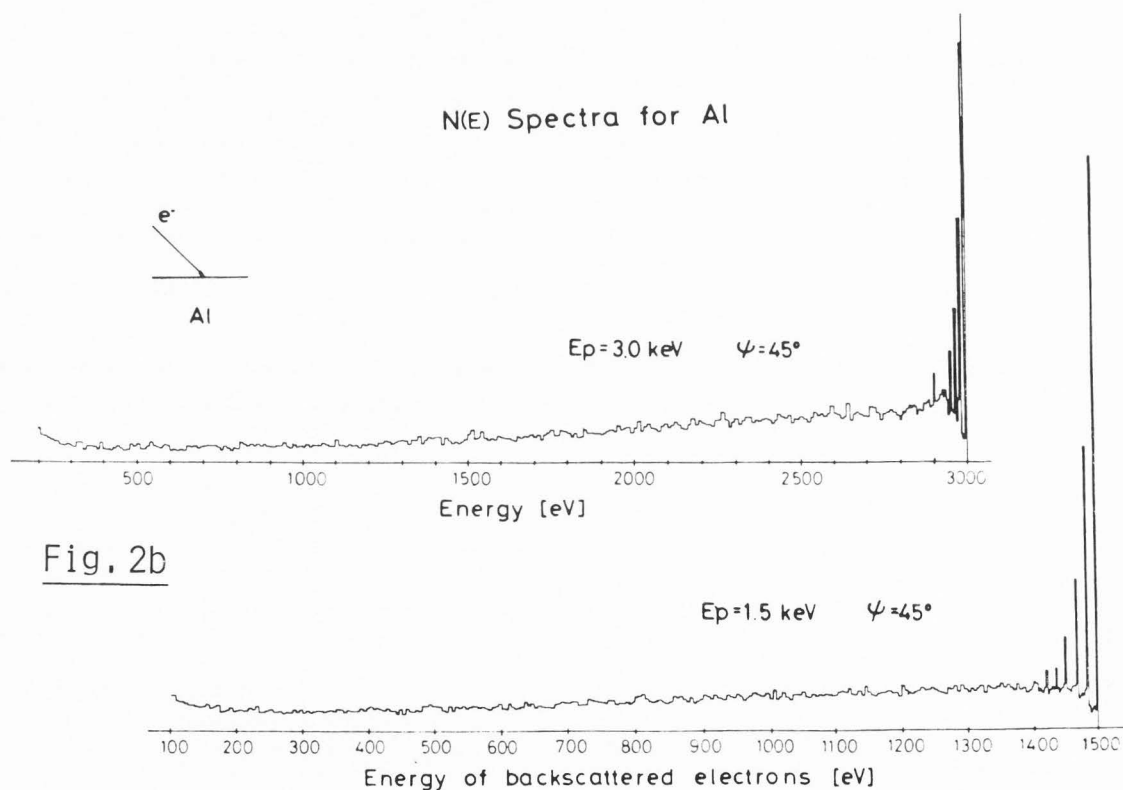
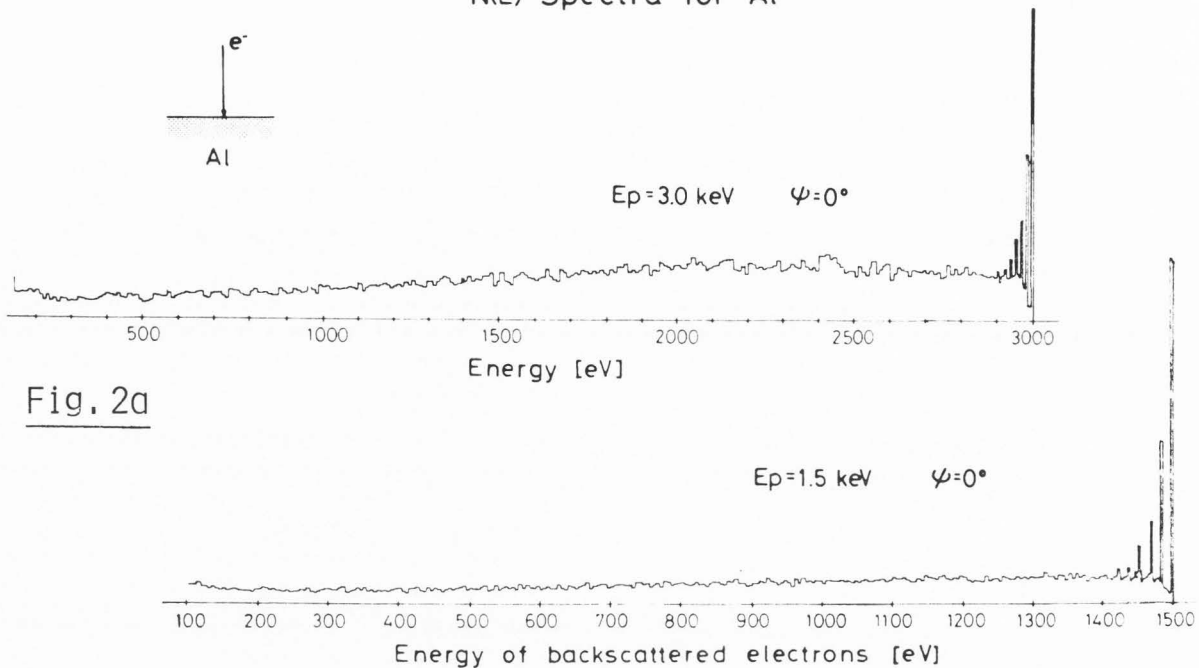


Fig. 2. Energy distribution of backscattered electrons (N(E)-spectrum) obtained from Monte Carlo calculations for $E_p = 1.5$ and 3.0 keV: (a) normal incidence, (b) angle of incidence 45° .

Theoretical N(E) Spectra for Aluminum

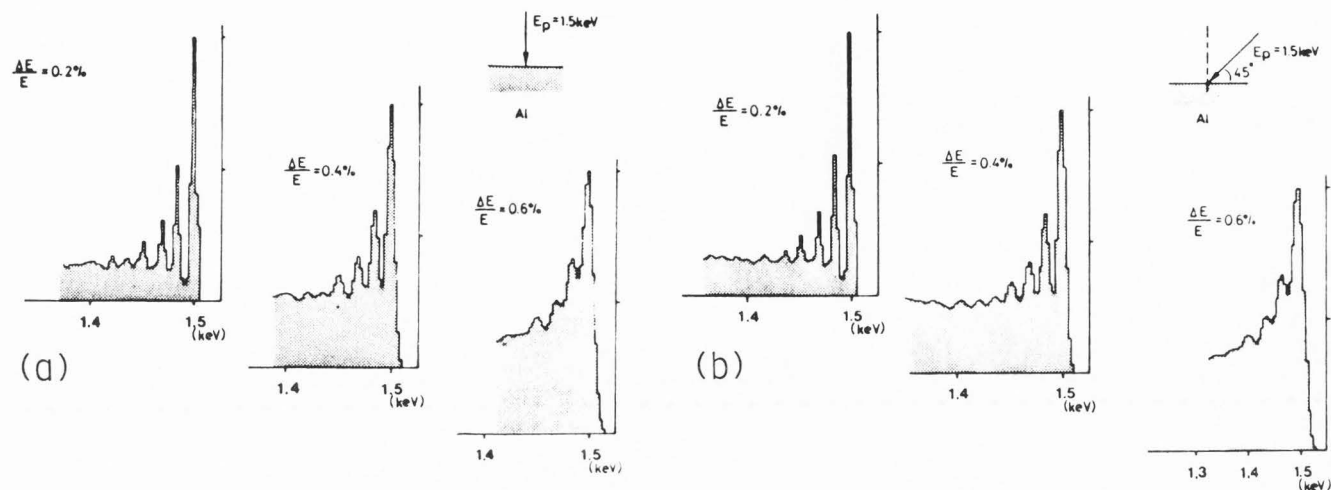


Fig. 3. Simulation of variation of N(E)-spectrum for different values of energy window of analyzer, ΔE , for $E_p = 1.5 \text{ keV}$; (a) normal incidence, (b) angle of incidence 45° .

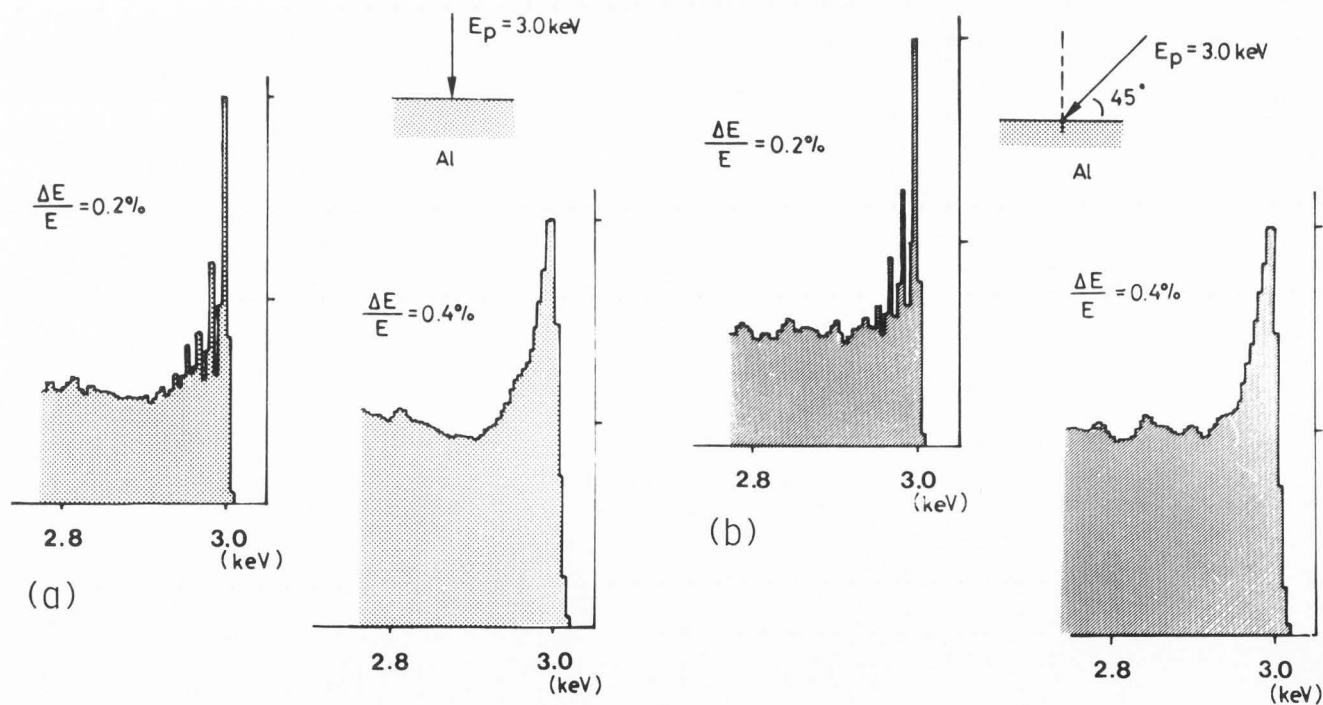


Fig. 4. Simulation of variation N(E)-spectrum for different values of energy window analyzer, ΔE , for $E_p = 3 \text{ keV}$; (a) normal incidence, (b) angle of incidence 45° .

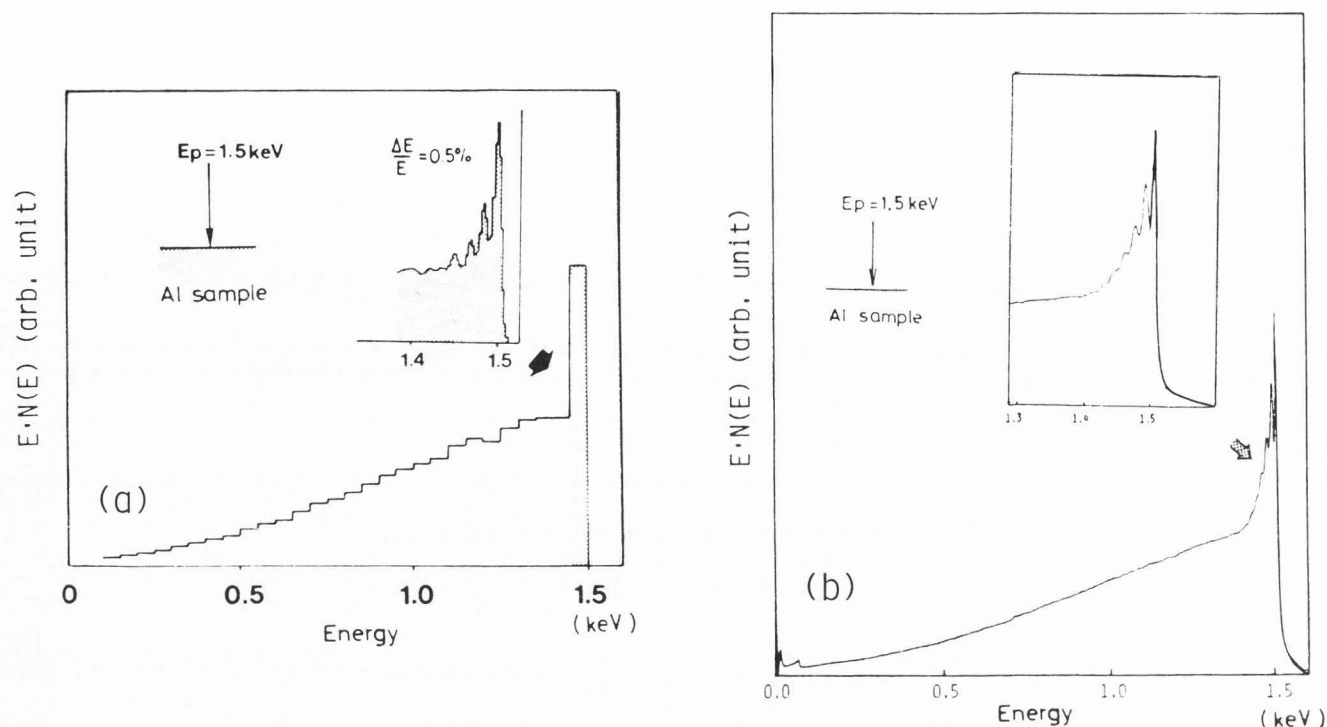


Fig. 5. $E \cdot N(E)$ -spectra for energy window of analyzer of $\Delta E/E = 0.5\%$ for $E_p = 1.5$ keV at normal incidence: (a) Monte Carlo simulation, (b) Experiment done with a scanning Auger electron microscope JAMP-10.

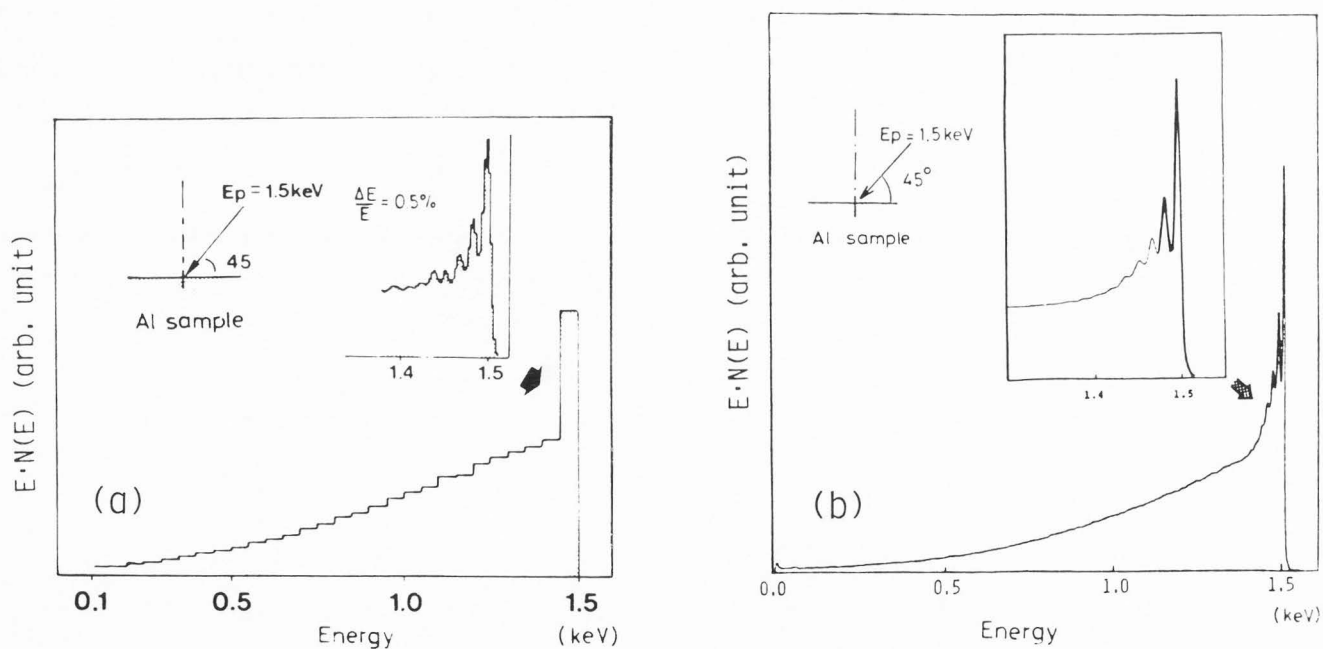


Fig. 6. $E \cdot N(E)$ -spectra for energy window of analyzer of $\Delta E/E = 0.5\%$ for $E_p = 1.5$ keV at angle of incidence 45° : (a) Monte Carlo simulation, (b) Experiment done with a scanning Auger electron microscope, JAMP-3.

Theoretical N(E) Spectra for Aluminum

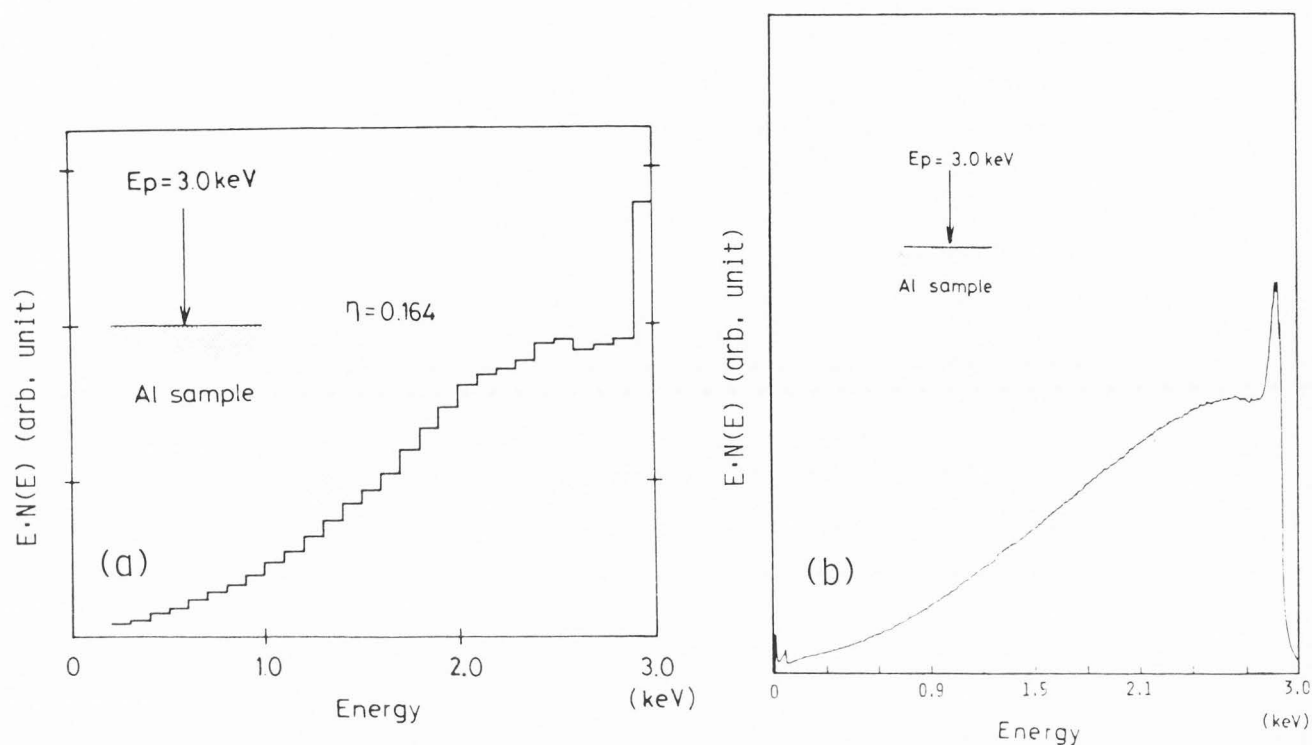


Fig. 7. E N(E)-spectra for energy window of analyzer of $\Delta E/E = 0.5\%$ for $E_p = 3 \text{ keV}$ at normal incidence: (a) Monte Carlo simulation, (b) Experiment done with a scanning Auger electron microscope JAMP-10.

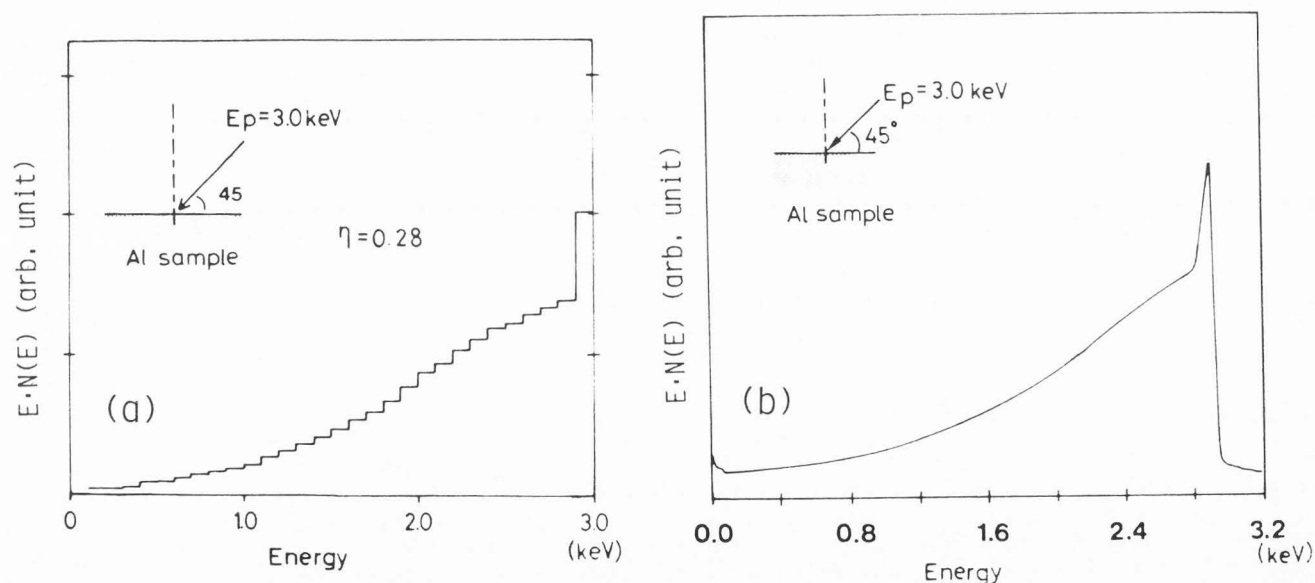


Fig. 8. E N(E)-spectra for energy window of analyzer of $\Delta E/E = 0.5\%$ for $E_p = 3 \text{ keV}$ at angle of incidence 45° : (a) Monte Carlo simulation, (b) Experiment done with a scanning Auger electron microscope, JAMP-3.

Acknowledgements

The authors are greatly indebted to Messrs. A. Mogami and T. Sekine of JEOL Co. for technical assistance in measuring the $E N(E)$ -spectra with the JAMP-10 and for stimulating discussion on the comparison between the theoretical and experimental results.

REFERENCES

- Ashley JC, Tung CJ and Richard RH. (1979). Electron inelastic mean free paths and energy losses in solids. *Surface Sci.*, **81**, 409-426.
- Gryzinski M. (1965). Two-Particle collision I, II, III. *Phys. Rev.*, **138**, A305-358.
- Ichimura S, Shimizu R. (1981). Backscattering correction for quantitative Auger analysis. I. Monte Carlo calculations of backscattering factors for standards materials. *Surface Sci.*, **112**, 386-407.
- Quinn JJ. (1962). Range of excited electrons in metals. *Phys. Rev.*, **126**, 1453-1457.
- Ritchie RH, Garber FW, Nakai MY and Birkhoff RD. (1969). Low energy electron mean free paths in solids. *Adv. Radiat. Biol.* (Academic Press, N.Y.) 1-28.
- Shimizu R, Kataoka Y, Ikuta T, Koshikawa T and Hashimoto H. (1976). A Monte Carlo approach to the direct simulation of electron penetration in solids. *J. Phys. D; Appl. Phys.*, **9**, 101-114.
- Streitwolf, HW. (1959). Zur Theorie der Sekundär Elektronen Emission von Metallen, Anregungsprozesse. *Ann. Phys. Leipzig* **3**, 183-196.
- Yamazaki Y. (1977). Studies on electron scattering by mercury atoms and electron spin polarization detector. PhD Thesis, Faculty of Engineering, Osaka University, Japan.